NASA TECHNICAL MEMORANDUM

NASA TM X-3153

NASA TM X-3153

TWO-DIMENSIONAL COLD-AIR CASCADE STUDY OF A FILM-COOLED TURBINE STATOR BLADE

II - Experimental Results of Full Film Cooling Tests

Herman W. Prust, Jr.

Lewis Research Center

Cleveland, Ohio 44135

NATIONAL AERONAUTICS AND SPACE ADMINISTRATION • WASHINGTON, D. C. • JANUARY 1975

1. Report No. NASA TM X-3153	2. Government Accession No.	3. Recipient's Catalog No.
4. Title and Subtitle TWO-DIMENSIONAL COLD-AIR CASCADE STUDY OF A FILM-COOLED TURBINE STATOR BLADE. II - EXPERIMENTAL RESULTS OF FULL FILM COOLING TESTS		5. Report Date January 1975 6. Performing Organization Code
7. Author(s) Herman W. Prust, Jr.		8. Performing Organization Report No. E-8052 10. Work Unit No. 501-24
9. Performing Organization Name and Address Lewis Research Center National Aeronautics and Space Administration Cleveland, Ohio 44135		11. Contract or Grant No. 13. Type of Report and Period Covered Technical Memorandum
12. Sponsoring Agency Name and Address National Aeronautics and Space Administration Washington, D.C. 20546		14. Sponsoring Agency Code

15. Supplementary Notes

16. Abstract

The effect of full film cooling on the performance of a turbine stator blade was studied in a two-dimensional cascade. The blade contained 12 rows of coolant holes, 6 rows on the suction surface and 6 on the pressure surface. Separate tests were first made with coolant ejection from each of the 12 rows. Then successive tests were made with various combinations of coolant rows open, including full film cooling. The principal results are presented in terms of primary-air efficiency as a function of coolant fraction. In addition, the efficiency results of the multirow tests are compared with the multirow efficiency predicted by adding the single-row results.

17. Key Words (Suggested by Author(s))
Turbine film-cooling
Aerodynamics
Cascades

18. Distribution Statement
Unclassified - unlimited
Category 01

19. Security Classif. (of this report)	20. Security Classif. (of this page)	21. No. of Pages	22. Price*
Unclassified	Unclassified	44	$3.75

* For sale by the National Technical Information Service, Springfield, Virginia 22151

TWO-DIMENSIONAL COLD-AIR CASCADE STUDY OF A FILM-COOLED TURBINE STATOR BLADE

II- EXPERIMENTAL RESULTS OF FULL FILM COOLING TESTS

by Herman W. Prust, Jr.

Lewis Research Center

SUMMARY

A systematic experimental investigation was conducted in a two-dimensional cascade to determine the effect on turbine stator blade performance of full film cooling from 12 spanwise rows of holes spaced over the blade surface. Six of the coolant rows were on the suction surface and six on the pressure surface. Tests were first made with coolant ejection from each of the 12 rows. Tests were next made with coolant ejection from various combinations of coolant rows, first on the pressure surface, then on the suction surface, and finally with full film cooling. The efficiency results of the multirow tests were then compared with the multirow efficiency predicted by adding the single-row results.

For the tested blading, the change in primary-air efficiency was essentially independent of primary-air velocity.

The location of the coolant row on the blade surface affected the change in primary-air efficiency. For instance, when the total pressure of the coolant in the blade cavity was equal to that of the inlet primary flow, the following percent changes in primary-air efficiency occurred per percent coolant flow:

(1) About 0.8 for coolant rows ejecting to surface static pressures higher than blade row exit static pressure, compared to about 0.4 for coolant rows ejecting to surface static pressures lower than blade row exit static pressure

(2) About 0.8 for coolant ejection from the six rows on the pressure surface, compared to about 0.5 for coolant ejection from the six rows on the suction surface

(3) About 0.6 for full film cooling from all 12 blade rows

Excellent agreement was obtained between experimental multirow primary-air efficiency and multirow efficiency predicted from adding experimental single-row results. Apparently, coolant ejected from an upstream row of holes did not affect the output of coolant ejected from downstream rows.

INTRODUCTION

Several analytical studies concerning the performance of cooled turbines (e.g., refs. 1 and 2) have shown that different means of ejecting compressor bleed coolant air from the turbine blade surface have significantly different effects on turbine efficiency.

Since high turbine efficiency is important in most engine designs, an extensive research program is in progress at the Lewis Research Center to investigate both experimentally and analytically the effect of different means of coolant ejection on turbine efficiency as well as on other aspects of turbine performance.

In recent years, several means of coolant ejection have been investigated. For instance, reference 3 reports the results of an experimental investigation conducted to determine the effect on stator blade performance of coolant ejection from four spanwise rows of coolant holes. The holes were located in or near the diffusion region on the suction surface at an angle of 35° to the blade surface. The axes of the holes were parallel to the end walls. References 4 to 6 report the results of experimental and analytical investigations of the influence on turbine stator and stage performance of turbine stator blade trailing-edge coolant ejection. And references 7 to 10 report the results of experimental and analytical investigations of the effect on turbine stator and stage performance of two types of stator blade transpiration discharge. (The referenced investigations were all conducted at coolant- to primary-air-temperature ratios near unity.) The results of the investigations of references 4 to 10 are summarized in reference 11.

The main conclusions of references 3 to 10 were (1) that coolant flow discharged from the suction surface in or near the diffusion region at an angle of 35° to the blade surface decreased the turbine work output at low coolant ejection velocities and increased the turbine work output at high coolant ejection velocities, (2) that coolant flow ejected from a trailing-edge slot parallel to the main stream significantly increased the turbine work output, and (3) that coolant flow ejected over the complete blade surface at an angle normal to the blade surface contributed little or nothing to the turbine work output.

The investigation described in this report is part of a continuing study of the effect of different means of stator blade full film cooling on turbine stator and stage performance. It concerns the effect on stator blade performance of full film coolant ejection from 12 spanwise rows of holes spaced over the blade surface. Six of the 12 rows were on the pressure surface and six were on the suction surface. The axes of the holes were located parallel to the end walls at various angles to the blade surface, as dictated by cooling and aerodynamic considerations.

The subject investigation is an extension of the investigation of reference 12, which reports the influence on stator blade performance of coolant ejection from six coolant

rows on the blade pressure surface. The results of reference 12 show that, with pressure-surface ejection, a significant portion of the ideal energy of the coolant results in useful kinetic energy at the blade row exit and that multirow performance can be predicted from single-row performance.

In the subject investigation to determine the effect of full film cooling on stator performance, the influence on stator performance of coolant discharge from each of the six rows of holes on the suction surface was first determined separately. Next, the effect of multirow ejection from the suction surface was determined. In the multirow investigation the combinations of coolant rows considered were the two rows nearest the blade leading edge, the three rows nearest the leading edge, etc., until all six rows on the suction surface were included. Finally, the influence on stator performance was determined for full film cooling from all 12 rows of coolant holes. In addition to these results the influence of coolant ejection from the four rows of coolant holes nearest the leading-edge stagnation point (shower head) - two rows on the suction surface and two rows on the pressure surface - was determined.

The testing for the subject report was conducted in a two-dimensional cascade. The temperatures of the primary and coolant air were nearly the same, atmospheric air being used as the primary air.

The single-row and multirow tests were conducted at nominal ideal primary-air exit critical velocity ratios of 0.5, 0.65, and 0.8. The range of coolant- to primary-air-mass-flow ratios investigated was from zero to about 0.04 from each coolant row.

The principal results are reported in terms of primary-air efficiency as a function of coolant fraction. Primary-air efficiency is defined as the ratio of the actual kinetic energy of the total flow to the ideal kinetic energy of the primary flow only, and the coolant fraction is defined as the ratio of coolant to primary-air mass flow.

In order to determine if coolant ejected from upstream rows of holes affects the output of coolant ejected from succeeding rows downstream, the primary-air efficiency results of the single-row tests were added and compared with the primary-air efficiency results of the multirow tests.

In addition to the principal results reported in the main text, experimentally determined values of coolant hole discharge coefficients, which are of engineering interest, are presented as an appendix.

The U.S. customary system of units was used in conducting the test reported herein. Conversion to the International System of Units (SI) was done for reporting purposes only.

APPARATUS, INSTRUMENTATION, AND PROCEDURE

Blading

Photographs of the test blading showing the 12 rows of coolant holes - 6 rows on the pressure surface and 6 rows on the suction surface - are presented in figure 1. As indicated, the blading is hollow and of constant cross section. The blade profiles correspond to the mean section profile of the stator blade of reference 13, in which the blades are described in detail. Significant dimensions of the blading are as follows: span, 10.16 centimeters (4.0 in.); chord, 5.74 centimeters (2.26 in.); pitch, 4.14 centimeters (1.63 in.).

The profile of the subject blading and the location, geometry, and numbering system of the coolant holes and rows are shown in figure 2 and table I. The axes of all coolant holes are parallel to the planes of the blade end surfaces. The diameter and pitch of the coolant holes in all rows are 0.076 centimeter (0.030 in.) and 0.114 centimeter (0.045 in.), respectively. Other pertinent data concerning the coolant holes are listed in table I. (The symbols used in table I are illustrated in fig. 2. All symbols are defined in appendix A.)

Cascade

The blading was tested in the simple two-dimensional cascade shown in figure 3. There are 12 blades in the cascade. However, only the three blades near the center are cooled. Other details of the cascade are described in reference 14. Primary (atmospheric) air enters the cascade inlet shown on the right in figure 3, and coolant air enters the inside of the three hollow blades near the center of the cascade through the coolant manifold and associated piping. The survey probe actuator indicated in figure 3 operates a slide in which a multipurpose survey probe is mounted downstream of the blading. The coolant and primary flow passing through the blading is discharged from the cascade through exhaust piping attached to the circular base of the cascade.

Instrumentation

A calibrated multipurpose survey probe of the type shown in figure 4 was used to determine the flow angle, the static pressure, and the loss in total pressure downstream of the blading. (A detailed description of this type of probe is given in ref. 14.) Coolant total pressure p'_c inside the blade was measured with a total pressure probe. The

sensing element of the probe was located 2.54 centimeters (1.0 in.) from the blade end wall on the coolant manifold side. The circular sensing end of the probe faced the coolant flow entering the blading so that the total pressure inside the blade was measured as accurately as was practical.

Coolant flow was measured by using calibrated sharp-edged orifice plates of various sizes located in an orifice run either 2.54 centimeters (1.0 in.) or 5.08 centimeters (2.0 in.) in diameter. The orifice runs, including instrumentation and orifice plates, all conformed to ASME specifications. All pressure data taken during survey tests were measured by using calibrated strain-gage transducers.

Test Procedure

When investigations for both single-row and multirow coolant discharge were conducted, three blades of the same profile with the same row or rows of coolant holes open were installed near the center of the cascade. Coolant air was then supplied to these blades only. Data were taken for only the center blade of the three test blades so that the measured data simulated data for a blade in a completely cooled blade row having adjacent blades of the same design and with the same flow conditions. Also to eliminate the effect of end wall conditions on the measurements, data were taken at the mean section of the blading only.

In order to operate the test facility, primary (atmospheric) air is caused to flow through the cascade by use of the laboratory altitude exhaust system, which is piped to the cascade outlet. Desired primary-air pressure ratios across the blade row are maintained by regulation of an exhaust control valve. Coolant airflow is provided by the laboratory combustion air system. Desired coolant flow rates were obtained by first setting the upstream orifice pressure with an upstream pressure regulator and then setting the pressure ratio across the orifice plate by regulating a throttling valve downstream of the orifice plate.

Before the blade survey testing was started, blade surface static pressures were determined from manometer board readings at primary-air ideal exit critical velocity ratios of 0.5, 0.65, and 0.8.

In order to conduct survey tests, the desired primary-air critical velocity ratio and coolant fraction were established for the blading by regulating the primary and coolant flow control valves. A survey was then made with the multipurpose probe across one blade pitch of the middle test blade to determine the downstream flow condition of the test blading. During the survey, all data, including survey data and coolant flow data, were digitized and recorded on magnetic tape. Also during testing, pertinent survey data were monitored on x-y recorders, and all data were monitored by teletype feedback from the laboratory data processing center.

The investigation of the test blading included survey tests with both single-row and multirow coolant ejection. Separate tests were first made with coolant ejection from each of the six single rows of coolant holes on the pressure surface. Then tests were made with coolant ejection from multiple coolant rows on the pressure surface. (The test results for coolant ejection from the pressure surface are reported in ref. 12.) In the multirow tests the combinations of rows considered were the two rows nearest the leading edge, the three rows nearest the leading edge, etc., until all six rows on the pressure surface were included. After the testing of coolant ejection from the pressure surface was completed, the same order of testing was used for single-row and multirow coolant ejection from the suction surface. After these systematic tests of coolant ejection from the suction and pressure surfaces, tests of full film cooling were made. In addition, multirow tests were conducted with coolant discharge from the four coolant rows nearest the leading edge. The multirow tests are listed in table II.

The survey investigations of both single-row and multirow coolant discharge were conducted at three nominal ideal primary-air exit critical velocity ratios $(V/V_{cr})_{p,id,m}$: 0.5, 0.65, and 0.8. For the single-row tests the range of coolant fractions investigated was from zero to about 0.04. For the multirow tests the range of coolant fractions investigated varied for the following reasons: With multirow discharge the minimum practical coolant fraction occurs when the total pressure inside the blade p'_c is a little higher than the blade surface pressure p_s of the coolant row nearest the leading edge of the blade. If the total pressure inside the blade is lower than the blade surface pressure of the coolant row nearest the leading edge, primary air flows abnormally into the interior of the blade through the row nearest the leading edge and out coolant rows farther downstream. Under these conditions a portion of the blade surface near the leading edge would, of course, not be film cooled. The minimum coolant fractions for multirow ejection were determined by this consideration. The maximum coolant fractions were determined by the number of coolant rows open with the total pressure inside the blade limited to about 13.9 N/cm^2 absolute (20 psia).

Calculation Procedure

The general procedure for computing the test results was as follows: Coolant fractions were computed by using the method specified in the ASME code for sharp-edged orifices. Local values of mass flow, momentum, flow angle, static pressure, and kinetic energy at each data point included in the survey were then computed. These local values were next integrated at the measuring station. Then, with conservation of mass and momentum assumed, the integrated values at the measuring station were equated to the same quantities at the hypothetical aftermixed downstream station. These equations

were then solved simultaneously to obtain the aftermixed flow conditions. (Equations for the survey data calculation procedure may be found in ref. 15.) With the aftermixed flow conditions known, the primary-air efficiency, as well as other results of interest, could be computed at fully mixed flow conditions.

Efficiency. - There are a number of efficiency expressions commonly used to describe the performance of high-temperature turbines requiring coolant. For cold aerodynamic tests with no internal inserts to duplicate actual hot-engine heat transfer or pressure drop processes, the selection becomes arbitrary. The major parameter studied in the subject aerodynamic tests was the effect of ejected coolant on the output kinetic energy of the combined flow (primary plus coolant). Therefore, primary-air efficiency was selected as the most direct form of efficiency to investigate changes in output energy as affected by adding coolant. Primary-air efficiency relates the actual kinetic energy of the total flow to the ideal energy of only the primary flow and is expressed as

$$\eta_{p,m} = \frac{w_t V_m^2}{w_p V_{p,id,m}^2} \tag{1}$$

and in terms of isolated flows is equivalent to

$$\eta_{p,m} = \frac{w_p V_{p,m}^2 + w_c V_{c,m}^2}{w_p V_{p,id,m}^2} \tag{2}$$

where $w_p V_{p,m}^2 / w_p V_{p,id,m}^2$ is the efficiency of the primary flow. Equation (1) was used to compute experimental results.

Thermodynamic efficiency is the same as primary-air efficiency except that the ideal energy of the coolant flow is included in the denominator. Because the stator blades have fixed holes, the only way to vary coolant flow is to vary the blade cavity pressure, which in turn varies the ideal energy of the coolant. The major reason primary-air efficiency was selected over thermodynamic efficiency, then, is that it reduces the number of variables to consider when studying the effect of coolant on output energy. If primary-air efficiency increases with coolant addition, the coolant flow causes the output of the total flow to be increased relative to the output of the uncooled primary flow. If primary-air efficiency remains unchanged, the net effect is that the coolant flow causes the output of the total flow to be the same as the output of the uncooled primary flow. If primary-air efficiency decreases, the net effect is that the coolant flow causes the output of the total flow to be reduced relative to the output of the

uncooled primary flow.

Prediction of multirow performance by addition of single-row data. - A commonly used method of presenting the effect of coolant on efficiency for both single-row (SR) and multirow (MR) tests is to plot the fractional change in primary-air efficiency $(\Delta\eta_p/\eta_o)_m$ against coolant fraction y, where $\Delta\eta_{p,m} = \eta_{p,m} - \eta_{o,m}$ and $\eta_{o,m}$ is the efficiency of the blade row with no coolant.

In predicting the multirow primary-air efficiency from the single-row primary-air efficiency, it is assumed that efficiency of the primary flow is unaffected by the coolant flow. Although it is recognized that this may not be true, it enables the interpretation of the results to be consistent with the use of primary-air efficiency (eq. (2)). That is, all changes in efficiency are attributed to the coolant flow. If the multirow efficiencies can be predicted from the single-row efficiencies by using the assumption that the efficiency of the primary flow is unaffected by the coolant flow, it would indicate either that the assumption is valid or that the net effect of the interaction between the coolant and primary flow energies is equivalent to assuming constant efficiency of the primary flow.

In adding the single-row data to predict multirow performance, the following assumptions were made concerning each given single-row condition applied to multirow conditions (see appendix A for definitions):

(1) Constant w_c for same cavity pressure

(2) Constant $V_{c,m}$ (no change in loss)

(3) Constant $V_{p,id,m}$ (same setting condition)

(4) Constant $V_{p,m}$ (no change in efficiency of primary air)

With these assumptions, the change in efficiency for the multirow case in terms of single-row conditions is calculated as follows: Equation (2) is rewritten (with assumptions 3 and 4) as

$$\eta_{p,m} = \eta_{o,m} + \frac{w_c V_{c,m}^2}{w_p V_{p,id,m}^2} \tag{3}$$

or

$$w_c V_{c,m}^2 = \Delta\eta_{p,m} w_p V_{p,id,m}^2 \tag{4}$$

For multirow conditions, assume rows 1 and 2 are open (indicated by the subscript 1+2). Rewriting equation (3) with assumptions 1 and 2 yields

$$\eta_{p(1+2),m} = \eta_{o,m} + \frac{w_{c,1}V^2_{c,1,m} + w_{c,2}V^2_{c,2,m}}{w_{p(1+2)}V^2_{p,id,m}}$$

then

$$\Delta\eta_{p(1+2),m} = \frac{(\Delta\eta_p)_{1,m} w_{p,1}V^2_{p,id,m} + (\Delta\eta_p)_{2,m} w_{p,2}V^2_{p,id,m}}{w_{p(1+2)}V^2_{p,id,m}}$$

and

$$\left(\frac{\Delta\eta_p}{\eta_o}\right)_{(1+2),m} = \frac{w_{p,1}}{w_{p(1+2)}}\left(\frac{\Delta\eta_p}{\eta_o}\right)_{1,m} + \frac{w_{p,2}}{w_{p(1+2)}}\left(\frac{\Delta\eta_p}{\eta_o}\right)_{2,m} \tag{5}$$

where subscripts 1 and 2 refer to single-row conditions of row 1 and row 2 and subscript (1+2) refers to multirow conditions when rows 1 and 2 are open. For the general multirow (MR) case with n rows open,

$$\left(\frac{\Delta\eta_p}{\eta_o}\right)_{MR,m} = \sum_{SR=1}^{SR=n}\left(\frac{w_{p,SR}}{w_{p,MR}}\right)\left(\frac{\Delta\eta_p}{\eta_o}\right)_{SR,m} \tag{6}$$

Similarly, the summation of coolant fractions (with assumption 1) is as follows. Again assuming rows 1 and 2 are open,

$$y_{(1+2)} = \frac{w_{c,1} + w_{c,2}}{w_{p(1+2)}} \tag{7}$$

or

$$y_{(1+2)} = \left(\frac{w_{c,1}}{w_{p,1}}\right)\left[\frac{w_{p,1}}{w_{p(1+2)}}\right] + \left(\frac{w_{c,2}}{w_{p,2}}\right)\left[\frac{w_{p,2}}{w_{p(1+2)}}\right]$$

$$= \left[\frac{w_{p,1}}{w_{p(1+2)}}\right] y_1 + \left[\frac{w_{p,2}}{w_{p(1+2)}}\right] y_2 \tag{8}$$

For the general case

$$y_{MR} = \sum_{SR=1}^{SR=n} \left(\frac{w_{p,SR}}{w_{p,MR}}\right) y_{SR} \tag{9}$$

RESULTS AND DISCUSSION

The results of the investigation are presented in three parts. The first part includes the stator efficiencies determined experimentally with coolant ejection from each of the six rows of coolant holes on the suction surface tested individually. The second part presents the stator efficiency determined experimentally with coolant ejection from various combinations of coolant rows, including full film cooling. (The results of single-row and multirow coolant ejection from the pressure surface are reported in ref. 12.) The third part compares the experimentally determined stator efficiencies of the multirow tests with those predicted by adding the results of the single-row tests.

The performance of the stator with single-row and multirow coolant ejection is given in terms of changes in primary-air efficiency with change in coolant flow. As mentioned previously, primary-air efficiency is used rather than thermodynamic efficiency because it is simpler to study factors that influence the output energy of the flow if the varying ideal energy of the coolant does not have to be considered.

Single-Row Experimental Efficiency

This part of the report is presented in two sections. First, the experimentally determined stator efficiencies for coolant ejection from each of the single rows on the suction surface are presented. Then, the experimentally determined results for the six

individual coolant rows on the suction surface are compared with those for the six individual rows on the pressure surface.

Suction-surface-discharge single-row experimental efficiency. - The variations in primary-air efficiency $\eta_{p,m}$ for the six single-row tests on the suction surface are shown in figure 5 over a range of coolant fractions y from 0 to about 0.04. Data are shown for each configuration for ideal exit velocity ratios of 0.5, 0.65, and 0.8. The efficiency of the single-row configurations with no coolant varied from about 0.965 to 0.975 over the range of primary-air Mach numbers tested. The results in figure 5 indicate that the change in primary-air efficiency with increased coolant flow was, in general, affected only slightly by primary-air exit critical velocity ratio.

Figure 5 also shows different trends of the change in primary-air efficiency with increased coolant fraction for different coolant rows. For instance, the results for the blading with the three rows nearest the blade leading edge (rows 7 to 9; fig. 2) show an increase in primary-air efficiency with increasing coolant fraction. The test results for the three rows nearest the blade trailing edge (rows 10 to 12) show a decrease in primary-air efficiency with low coolant fractions and then a sharp increase in primary-air efficiency as the coolant fraction was increased.

The different trends of change in primary-air efficiency with increased coolant fraction for different coolant rows are shown more clearly when normalized to each of their respective zero-coolant-flow cases. Such a relation is shown in figure 6, where the fractional change in primary-air efficiency is compared to zero-coolant-flow efficiency $(\Delta\eta_p/\eta_o)_m$ as a function of coolant fraction y. (The results in the figure are average results computed from fig. 5 for the three tested primary-air critical velocity ratios.)

The change in primary-air efficiency that occurs when the total pressure of the coolant in the blade cavity is equal to the primary-air inlet total pressure is also of interest for the different coolant rows in figure 6. For these conditions, the average percent change in primary-air efficiency per percent coolant flow was about 0.6 for the three rows nearest the leading edge and about 0.4 for the three rows nearest the trailing edge. The average value was about 0.5 for all six rows on the suction surface.

Possible reasons for the different effects of coolant flow on primary-air efficiency for the different blade rows are discussed in the next section, which compares the effect of coolant flow on efficiency for suction- and pressure-surface single-row coolant discharge.

Effect of coolant discharge on primary-air efficiency for individual coolant rows on the suction and pressure surfaces of the blading. - A comparison of the individual effects on efficiency of each of the 12 coolant rows included in the test blading is useful if means of minimizing coolant flow loss are considered. Figure 6 presents the variations in primary-air efficiency with coolant fraction for the six rows on the suction surface, and

figure 7 presents similar results for the six rows on the pressure surface. (The results in fig. 7 are taken from ref. 12.)

Figures 6 and 7 indicate a significantly larger change in primary-air efficiency with coolant fraction for rows 1 to 9 than for rows 10 to 12. For example, when the total pressure of the coolant flow in the blade cavity and the inlet primary flow are equal, the average percent change in primary-air efficiency per percent coolant flow is about 0.8 for rows 1 to 9 and only about 0.4 for rows 10 to 12. Also as the total pressure of the coolant flow in the blade cavity was further increased above that of the inlet primary flow, with a corresponding increase in coolant fraction, the slope of fractional change in primary-air efficiency with coolant fraction increased for all the blade rows except 1 and 7. Therefore, as the total pressure in the blade cavity was increased above that of the inlet primary flow, the average percent change in primary-air efficiency per percent coolant flow increased for all blade rows, except rows 1 and 7.

The apparent reason for the significant difference in change in efficiency between rows 1 to 9 and rows 10 to 12 is indicated in figure 8, which shows the comparative blade surface static pressures for the 12 coolant rows. The figure shows that for rows 1 to 9 the coolant flow is discharged in the expansion region on the blade surface, and for rows 10 to 12 the coolant flow is discharged in the diffusion region on the blade surface. It therefore appears that coolant flow discharged in the diffusion region experiences higher losses because of diffusion, turning to the main flow direction, etc., than coolant discharged in the expansion region of the blade surface.

The preceding discussion concerning reasons for differences in efficiency changes for the different blade rows is a simplified one which does not include all known effects on efficiency, such as coolant ejection angle and possible effects on boundary layer, as well as other influences that may not be recognized at this time. For instance, the smaller change in primary-air efficiency of rows 1 and 7 relative to the other coolant rows, excepting row 6, in the upper range of coolant fraction, apparently results from the fact that the ejection angles for these rows are perpendicular to the blade surface, while the ejection angles for the other rows are at acute angles to the blade surface (table I). As a result, for rows 1 and 7, the dynamic head of the coolant at the coolant row exit is lost; for the other rows, a large portion of the dynamic head is recovered.

Multirow Experimental Efficiency

The multirow experimental efficiency results are presented as follows: First, the experimental results for coolant ejection from various combinations of rows on the suction surface are presented and compared. Next, the full film cooling results are shown and compared with results for coolant ejection from the suction surface only and also

with results for coolant ejection from the pressure surface only. Finally, results for coolant ejection from the four rows nearest the leading edge are presented; two of the rows were on the suction surface and two on the pressure surface.

Suction-surface-discharge multirow experimental efficiency. - Figure 9 presents the experimental change in primary-air efficiency as a function of coolant fraction for the various combinations of rows tested. The minimum points on the curves indicate the minimum amount of coolant that can be ejected without inflow of primary air through the coolant row nearest the leading edge (row 7). The results show that the primary-air critical velocity ratios considered had only a minor effect on the change in primary-air efficiency. The results also show an increase in primary-air efficiency with increasing coolant fraction for all combinations of coolant rows.

In figure 10, a comparison is shown of the fractional change in primary-air efficiency as a function of coolant fraction for coolant discharge from various combinations of coolant rows on the suction surface. (The results shown in fig. 10 are average results from fig. 9.) The results show that for a given coolant fraction there was a decrease in fractional change in primary-air efficiency as an increasing number of coolant rows, starting at the blade leading edge, were opened.

The reasons for the decrease in primary-air efficiency, at a given value of coolant fraction, as an increasing number of rows on the suction surface were opened were indicated in the previous discussion concerning the effect of coolant discharge on primary-air efficiency from single rows. The principal reason is that for the same total pressure in the blade cavity, the percent change in primary-air efficiency per percent coolant flow is, on the average, significantly larger for coolant discharge from rows which discharge in the expansion region of the blade surface than from rows which discharge in the diffusion region of the blade surface. The secondary reason for the decrease in primary-air efficiency at a given coolant fraction, as an increasing number of coolant rows were opened, is that to maintain a constant coolant fraction, the total pressure of the coolant flow in the blade cavity must be reduced as an increasing number of coolant rows are opened. As previously discussed with regard to the effect of coolant discharge on primary-air efficiency from single rows, the percent change in output per percent coolant flow decreased for all coolant rows, except rows 1 and 7, as the total pressure of the coolant flow in the blade cavity was reduced.

Therefore, for a given coolant fraction, as an increasing number of suction-surface coolant rows starting at the blade leading edge were opened, the fractional change in primary-air efficiency decreased as a result of both the decreasing percent change in efficiency per percent coolant flow for coolant rows farther from the leading edge and also the decreasing pressure of the coolant in the blade cavity.

The results in figure 10 also show that when the total pressure of the coolant in the blade cavity and the inlet primary flow were equal, as an increasing number of coolant

rows were opened, the percent change in primary-air efficiency per percent coolant flow decreased from about 0.6 for coolant discharge from rows 7 to 8 to about 0.5 for coolant discharge from rows 7 to 12. The reason for the decreasing percent change in primary-air efficiency for these conditions was discussed in the previous paragraph. When the total pressure of the coolant in the blade cavity was constant, the percent change in primary-air efficiency per percent coolant flow was, on the average, significantly larger for coolant discharge from rows which discharged in the expansion region of the blade surface than for rows which discharged in the diffusion region of the blade surface. With constant coolant cavity pressure, there was therefore a decrease in primary-air efficiency as an increasing number of blade rows, starting at the blade leading edge, were opened.

Full-film-cooling experimental efficiency. - The variation in primary-air efficiency with coolant flow for the stator blade with full film cooling is shown in figure 11. Figure 11(a) presents the experimental change in primary-air efficiency as a function of coolant fraction, and figure 11(b) presents the fractional change in primary-air efficiency relative to the uncooled blading as a function of coolant fraction.

The results in figure 11(a) for full film cooling show little or no effect of primary-air critical velocity ratio, and the change in primary-air efficiency is seen to increase with increasing coolant flow.

A comparison of the fractional change in primary-air efficiency for coolant discharge from the six rows on the suction surface and the six rows on the pressure surface with the fractional change in primary-air efficiency with full film cooling is revealing. This comparison is made in figure 12. The results show that for all values of coolant flow, the fractional change in primary-air efficiency was less for suction-surface coolant discharge than for pressure-surface discharge and still less for full-film-cooling discharge.

The general reasons for the larger increase in primary-air efficiency for coolant discharge from the six rows on the pressure surface than for the six rows on the suction surface have been discussed previously in this report.

The average coolant discharge pressure on the blade pressure surface was shown to be larger than that on the suction surface (fig. 8). Therefore, to maintain a given value of coolant fraction for coolant discharge from both the suction and pressure surfaces, the total pressure of the coolant flow in the blade cavity must be larger for pressure-surface discharge than for suction-surface discharge.

As previously discussed, for the same coolant total pressure in the blade cavity, the percent change in primary-air efficiency per percent coolant flow was larger for coolant discharge from the expansion region on the blade pressure surface than for coolant discharge from the diffusion region on the blade suction surface. Also, as previously mentioned, as the total pressure of the coolant in the blade cavity was increased,

the percent change in primary-air efficiency per percent coolant flow increased. Therefore, at the same coolant fraction, the average fractional change in primary-air efficiency was larger for coolant discharge from the pressure surface than from the suction surface as a result of the generally larger percent change in primary-air efficiency and higher coolant cavity pressure with pressure-surface discharge.

The reason for the smaller change in primary-air efficiency with full film cooling than with discharge from either the suction or pressure surface for the same coolant fraction (fig. 12) can be explained as follows: When the total pressure of the coolant flow was equal to that of the primary flow, the percent change in primary-air efficiency per percent coolant flow was about 0.8 for pressure-surface discharge and about 0.5 for suction-surface discharge. For these conditions the average percent change in primary-air efficiency per percent coolant flow for the suction and pressure surfaces is then about 0.6. For full film cooling, for the same coolant total pressure, the percent change in primary-air efficiency per percent coolant flow would be expected to be about equal to the average for the suction and pressure surfaces. The results in figure 12 show this to be true. For full film cooling, when the total pressure of the coolant flow was equal to the total pressure of the primary flow, the percent change in primary-air efficiency per percent coolant flow was about 0.6, the average of the suction- and pressure-surface values. Of course, with constant coolant total pressure, the total coolant fraction for full film cooling was larger than the coolant fraction of either the suction or pressure surfaces. As a consequence, for this case, when plotted as a function of coolant fraction, the change in primary-air efficiency for full film cooling was lower than that for coolant discharge from either the suction or pressure surface.

Experimental efficiencies for coolant discharge from four rows nearest the blade leading edge. - The variation in primary-air efficiency with coolant ejection from the four rows nearest the leading edge (rows 1, 2, 7, and 8) is shown in figure 13. Figure 13(a) presents the experimentally determined primary-air efficiency as a function of coolant fraction, and figure 13(b) presents the fractional variation in primary-air efficiency relative to the efficiency of the noncooled blade as a function of coolant fraction. As with the results for coolant discharge from other rows, the results indicate little effect of primary-air critical velocity ratio on the change in efficiency. The results show an increase in primary-air efficiency for all values of coolant fraction. When the total pressures of the coolant in the blade cavity and the inlet primary flow were equal, the percent change in primary-air efficiency per percent coolant flow (fig. 13(b)) was about 0.7. In other words, the effectiveness of the coolant was a little less than the average effectiveness of 0.8 for coolant ejected from all rows on the pressure surface.

Comparison of Additive Single-Row Results With Multirow Results

In order to determine if the coolant ejected from upstream coolant rows on the suction surface affects the performance of coolant ejected from succeeding holes downstream, the results of the single-row experimental tests were added and compared with the results of the multirow tests by using the equations given in the section Calculation Procedure and the method described in reference 12. To use this method requires that both the effect of cavity pressure on coolant flow from the different rows and the effect of coolant flow on primary flow be known. The effect of cavity pressure on the coolant flow for the various rows of holes on the suction surface is presented first. Next the effect of coolant flow on primary flow is shown. Finally, the additive results of the single-row tests are compared with the results of the multirow tests.

Effect of cavity pressure on coolant flow from suction-surface rows. - In figure 14, the fractional coolant flow y ejected from the different coolant rows on the suction surface of the blading is presented as a function of the pressure coefficient k_p. (Similar results are reported in ref. 12 for coolant ejection from the pressure surface.) The pressure coefficient k_p relates the cavity-total- to blade-exit-static-pressure drop of the coolant flow to the blade-inlet-total- to blade-exit-static-pressure drop of the primary flow.

The results in figure 14 show an increase in coolant fraction with increasing k_p for all blade rows, as expected, since with increasing k_p the total pressure of the coolant and the pressure drop across the coolant row increased. The results also show, except for rows 7 and 9 in the upper range of k_p's, that for constant k_p the coolant fraction for the different rows increased with decreasing blade surface pressure (fig. 9). This general trend, of course, occurred because of the larger pressure drop across the coolant rows with the lower surface pressures. The exceptions noted for rows 7 and 9 are probably attributable to significant differences in ejection angle and/or length-diameter L/D ratio of these two rows relative to the other rows (table I). Although the curves in figure 14 are indicated to be for an ideal primary-air exit critical velocity ratio of 0.65, they are also valid for ratios of 0.5 and 0.8.

Effect of coolant flow on primary flow. - The reduction in primary flow resulting from coolant discharge is shown in figure 15. Figure 15(a) presents the reduction in primary flow due to single-row and multirow coolant discharge from the suction surface. Figure 15(b) presents the reduction in primary flow due to coolant discharge from the four rows nearest the leading edge. And figure 15(c) shows the reduction in primary flow due to full film cooling. The curves shown are averaged curves obtained from data at the three tested ideal primary-air exit critical velocity ratios. As shown, the reduction in primary flow due to coolant discharge is significant. For coolant discharge from the suction surface (fig. 15(a)) there was an average reduction in primary flow of about 0.85 percent per percent coolant flow. For coolant discharge from the four rows near-

est the blade leading edge (fig. 15(b)) there was an average reduction in primary flow of about 1.0 percent per percent coolant flow. For full-film-cooling discharge (fig. 15(c)) the average reduction in primary flow varied with coolant flow. In the lower range of coolant flow, there was an average reduction in primary flow of about 1.2 percent per percent coolant flow. In the upper range of coolant flow, there was an average reduction in primary flow of about 0.75 percent per percent coolant flow.

Comparison of experimental multirow results with multirow results predicted from single-row experimental results. - Experimental multirow efficiency variations are compared with multirow efficiency variations predicted from single-row experimental results in figure 16. The curves shown for the multirow experimental results are average curves for the three primary-air exit critical velocity ratios considered, and the predicted multirow results are for a primary-air exit critical velocity ratio of 0.65 - the average of the three tested primary-air critical velocity ratios considered. (The predicted results at the other primary-air critical velocity ratios considered would be essentially the same as those for 0.65, except that the upper limit for the predicted coolant fraction would have been somewhat smaller for results at 0.8 and somewhat larger for results at 0.5.)

Figure 15 shows the fractional variation in multirow efficiency predicted from experimental single-row results to be less than about 0.01 different than the actual experimental multirow efficiency variations for all combinations of coolant rows tested. The results, therefore, strongly indicate that, for the tested stator blade, coolant ejected from upstream rows of holes did not significantly affect the output of coolant ejected from coolant rows farther downstream.

SUMMARY OF RESULTS

A systematic experimental investigation was conducted to determine the effect on turbine stator blade performance of full film cooling from 12 spanwise rows of holes spaced over the blade surface. Six of the 12 coolant rows were on the suction surface and the other six were on the pressure surface. The axes of the holes were located parallel to the end walls at various angles with the blade surface as dictated by aerodynamic and cooling considerations.

The following order of testing was used in conducting the systematic investigation: The effect on stator performance of coolant ejection from the 12 individual rows was first determined. Next, the effect of multirow ejection from various combinations of coolant rows on the pressure surface, starting with the rows nearest the blading leading edge, was investigated. Then the effect of multirow ejection from the suction surface was investigated for similar combinations of coolant rows as those investigated for the

pressure surface. Finally, the influence on stator blade performance of full film cooling from all 12 rows of holes was investigated. In addition, the influence of coolant ejection from the four rows of holes nearest the leading-edge stagnation point (shower head) was determined. (All results concerning the investigation of coolant discharge from the pressure surface of this blading are reported in ref. 12.)

Also, to ascertain if coolant flow ejected from upstream rows of holes affects the performance of coolant flow ejected from succeeding rows downstream, the performance results of the single-row tests were added and compared with the multirow test results.

The tests were conducted in a two-dimensional cascade with the coolant and primary-air temperatures essentially equal to atmospheric. All configurations were tested at three nominal ideal exit primary-air critical velocity ratios of 0.5, 0.65, and 0.8.

The results are reported principally in terms of primary-air efficiency as a function of coolant fraction. Primary-air efficiency is defined as the ratio of the actual kinetic energy of the total flow relative to the ideal energy of the primary flow only, and the coolant fraction is defined as the ratio of the coolant mass flow to the primary-air mass flow.

The results are summarized as follows:

1. For the tested blading, the fractional change in primary-air efficiency was only slightly affected by primary-air ideal exit critical velocity ratio.

2. With single-row coolant ejection, the fractional change in primary-air efficiency was influenced primarily by the amount of the coolant flow and the location of the coolant rows. For coolant rows having blade surface exit static pressures higher than blade row exit static pressure, the primary-air efficiency increased with increasing values of coolant fraction. For coolant rows having blade surface exit static pressures lower than blade row exit static pressure (in the diffusion region on the blade surface), the primary-air efficiency first decreased with increasing coolant fraction and then increased as the coolant fraction was further increased. When the total pressure of the coolant in the blade cavity was equal to the total pressure of the primary flow at the inlet, the average percent change in primary-air efficiency per percent coolant flow was about 0.8 for the rows having blade surface exit static pressures higher than blade row exit static pressure and about 0.4 for the rows having blade surface exit static pressures lower than blade row exit static pressure.

3. With multirow coolant ejection from the suction surface, there was an increase in primary-air efficiency with coolant fraction for coolant ejection from all combinations of rows starting at the leading edge. When the total pressure of the coolant in the blade cavity was equal to the primary-air inlet total pressure, the percent change in primary-air efficiency per percent coolant flow was about 0.6 when the two rows nearest the leading edge were open, decreasing to about 0.5 when all six rows were open.

4. With full film cooling, the primary-air efficiency increased with increasing coolant flow. When the total pressure of the coolant in the blade cavity was equal to the primary-air inlet total pressure, the percent change in primary-air efficiency per percent coolant flow was about 0.6. This percent change in primary-air efficiency for full film cooling compares with a change of about 0.8 for ejection from the six rows on the pressure surface and a change of about 0.5 for ejection from the six rows on the suction surface.

5. With coolant ejection from the four rows nearest the blade leading edge, the primary-air efficiency increased with increased coolant flow. When the total pressures of the coolant in the blade cavity and the inlet primary flow were equal, the percent change in primary-air efficiency per percent coolant was about 0.7.

6. The results of the investigation for this blading show that changes in experimentally determined values of multirow primary-air efficiency can be predicted by properly adding the single-row changes in primary-air efficiency. Apparently, coolant ejection from upstream rows of coolant holes did not affect the output of coolant ejected from one or more coolant rows downstream.

Lewis Research Center,
National Aeronautics and Space Administration,
Cleveland, Ohio, September 11, 1974,
501-24.

APPENDIX A

SYMBOLS

A area, m^2; ft^2

C_D discharge coefficient, ratio of actual flow to ideal flow

D diameter of coolant hole, cm; in.

k_p pressure coefficient, $(p'_c - p_m)/(p'_{p,0} - p_m)$

L coolant hole length, cm; in.

L_{pr} pressure-surface length from leading edge to trailing edge (fig. 2), cm; in.

L_s suction-surface length from leading edge to trailing edge (fig. 2), cm; in.

n number of coolant rows open

p absolute pressure, N/cm^2; psia

Re Reynolds number

T absolute temperature, K; ^oR

V absolute velocity, m/sec; ft/sec

w mass flow rate, kg/sec; lbm/sec

x local position along blade surface from leading edge (fig. 2), cm; in.

y coolant fraction, w_c/w_p

β angle between coolant hole axis and local blade surface tangent in plane parallel to blade end surface, deg

η_o blade-row efficiency with no coolant flow

η_p primary-air efficiency, ratio of kinetic energy of total flow to ideal kinetic energy of primary flow only

μ viscosity, $N\text{-sec}/m^2$; lbm/sec-ft

ρ density, kg/m^3; lbm/ft^3

Subscripts:

c coolant flow

cr conditions at Mach 1

h coolant hole

id ideal quantity corresponding to isentropic process

MR conditions for multirow of coolant holes open

m station at blade exit where flow conditions are assumed to be uniform

o conditions with no coolant flow

p primary flow

SR conditions for single-row coolant holes open

s blade surface conditions

0 station at blade row inlet

Superscript:

' total-state conditions

APPENDIX B

COOLANT HOLE DISCHARGE COEFFICIENTS

This appendix presents the coolant hole discharge coefficients for each of the six different suction-surface coolant hole configurations tested. (See ref. 12 for pressure-surface coolant hole discharge coefficients.) The discharge coefficients are presented as a function of both ideal coolant hole Reynolds number and primary-air exit critical velocity ratio.

The discharge coefficients are, of course, the ratio of the actual to the ideal flow through the coolant hole. Thus,

$$C_{D,h} = \frac{w_{c,h}}{(\rho V)_{id,h}} A_h \tag{B1}$$

The actual coolant flow per hole $w_{c,h}$ was determined by using sharp-edged-orifice data.

The upstream flow conditions used for the determination of the ideal density and velocity at the exit of the hole were obtained from the measured total pressure p'_c and total temperature T'_c inside the blade. The downstream flow conditions used for the determination of the ideal density and velocity at the exit of the hole were obtained from the measured blade surface static pressure at the location of the coolant hole p_s.

The ideal Reynolds numbers based on hole diameter were computed from the standard relation

$$Re_{id,h} = \frac{(\rho V)_{id,h} D}{\mu} \tag{B2}$$

Figure 17 presents the coolant hole discharge coefficients as a function of both ideal Reynolds number and ideal primary-air exit critical velocity ratio for the six different coolant rows. In addition, in figure 8 the ratios of blade surface static pressure to inlet total pressure at the different coolant row locations are presented as a function of blade surface length for a primary-air ideal exit critical velocity ratio of 0.65. (These pressure ratios are presented for completeness in case the reader might wish to use the experimental data for other calculations.)

In figure 17, the discharge coefficients are shown to vary with Reynolds number and primary-air critical velocity ratio. The maximum discharge coefficients, at the maximum Reynolds number considered, varied from about 0.70 to 0.75 for the different hole

configurations. In general, for all hole configurations, the discharge coefficients decreased with decreasing Reynolds number. At the higher Reynolds numbers, the coefficients were, in general, affected only slightly by primary-air critical velocity; however, as the Reynolds number decreased from the maximum considered, the coefficients for all configurations were affected to some degree by primary-air critical velocity ratio. The general trend of coefficients at the lower Reynolds numbers is to decrease with increasing primary-air critical velocity ratio; however, for some of the rows of coolant holes, there are exceptions to this general trend.

REFERENCES

1. Hartsell, J. E.: Prediction of Effects of Mass-Transfer Cooling on the Blade-Row Efficiency of Turbine Airfoils. Paper 72-11, AIAA, Jan. 1972.

2. Prust, Herman W., Jr.: An Analytical Study of the Effect of Coolant Flow Variables on the Kinetic Energy Output of a Cooled Turbine Blade Row. Paper 72-12, AIAA, Jan. 1972.

3. Brown, Douglas B.; and Helon, Ronald M.: Cold-Air Aerodynamic Study in a Two-Dimensional Cascade of a Turbine Stator Blade With Suction-Surface Film Cooling. NASA TM X-2685, 1973.

4. Whitney, Warren J.; Szanca, Edward M.; and Behning, Frank P.: Cold-Air Investigation of a Turbine With Stator-Blade Trailing-Edge Coolant Ejection. I - Overall Stator Performance. NASA TM X-1901, 1969.

5. Prust, Herman W., Jr.; Behning, Frank P.; and Bider, Bernard: Cold-Air Investigation of a Turbine With Stator-Blade Trailing-Edge Coolant Ejection. II - Detailed Stator Performance. NASA TM X-1963, 1970.

6. Szanca, Edward M.; Schum, Harold J.; and Prust, Herman W., Jr.: Cold-Air Investigation of a Turbine With Stator-Blade Trailing-Edge Coolant Ejection. III - Overall Stage Performance. NASA TM X-1974, 1970.

7. Prust, Herman W., Jr.; Schum, Harold J.; and Szanca, Edward M.: Cold-Air Investigation of a Turbine With Transpiration-Cooled Stator Blades. I - Performance of Stator With Discrete Hole Blading. NASA TM X-2094, 1970.

8. Szanca, Edward M.; Schum, Harold J.; and Behning, Frank P.: Cold-Air Investigation of a Turbine With Transpiration-Cooled Stator Blades. II - Stage Performance With Discrete Hole Stator Blades. NASA TM X-2133, 1970.

9. Behning, Frank P.; Prust, Herman W., Jr.; and Moffitt, Thomas P.: Cold-Air Investigation of a Turbine With Transpiration-Cooled Stator Blades. III - Performance of Stator With Wire-Mesh Shell Blading. NASA TM X-2166, 1971.

10. Behning, Frank P.; Schum, Harold J.; and Szanca, Edward M.: Cold-Air Investigation of a Turbine With Transpiration-Cooled Stator Blades. IV - Stage Performance With Wire-Mesh Shell Stator Blading. NASA TM X-2176, 1971.

11. Moffitt, Thomas P.; Prust, Herman W., Jr.; Szanca, Edward M.; and Schum, Harold J.: Summary of Cold-Air Tests of a Single-Stage Turbine With Various Cooling Techniques. NASA TM X-52968, 1971.

12. Moffitt, Thomas P.; Prust, Herman W., Jr.; and Bartlett, Wayne M.: Two-Dimensional Cold-Air Cascade Study of a Film-Cooled Turbine Stator Blade. I - Experimental Results of Pressure-Surface Film Cooling Tests. NASA TM X-3045, 1974.

13. Whitney, Warren J.; Szanca, Edward M.; Moffitt, Thomas P.; and Monroe, Daniel E.: Cold-Air Investigation of a Turbine for High-Temperature-Engine Application. I - Turbine Design and Overall Stator Performance. NASA TN D-3751, 1967.

14. Stabe, Roy G.: Design and Two-Dimensional Cascade Test of Turbine Stator Blade With Ratio of Axial Chord to Spacing of 0.5. NASA TM X-1991, 1970.

15. Goldman, Louis J.; and McLallin, Kerry L.: Cold-Air Annular-Cascade Investigation of Aerodynamic Performance of Cooled Turbine Vanes. I - Facility Description and Base (Solid) Vane Performance. NASA TM X-3006, 1974.

TABLE I. - COOLANT HOLE DATA

Coolant row	Percent of blade surface length, x/L_{pr} or x/L_s	Angle between coolant hole axis and local blade surface tangent in plane parallel to blade end surfaces, β, deg	Length-diameter ratio of coolant hole, L/D
1	3.5	90	2.2
2	12	34	3.7
3	20	33	3.3
4	45	35	
5	70	33	
6	85	34	
7	3.5	90	2.2
8	10.5	36	3.7
9	20	39	4.5
10	40	38	4.0
11	60	38	3.8
12	80	35	3.8

TABLE II. - LISTING OF MULTIROW

COOLANT TESTS

Multirow configurations tested	Coolant rows included
1	1, 2
2	1, 2, 3
3	1, 2, 3, 4
4	1, 2, 3, 4, 5
5	1, 2, 3, 4, 5, 6
6	7, 8
7	7, 8, 9
8	7, 8, 9, 10
9	7, 8, 9, 10, 11
10	7, 8, 9, 10, 11, 12
11	1, 2, 7, 8,
12	1 to 12 (full film)

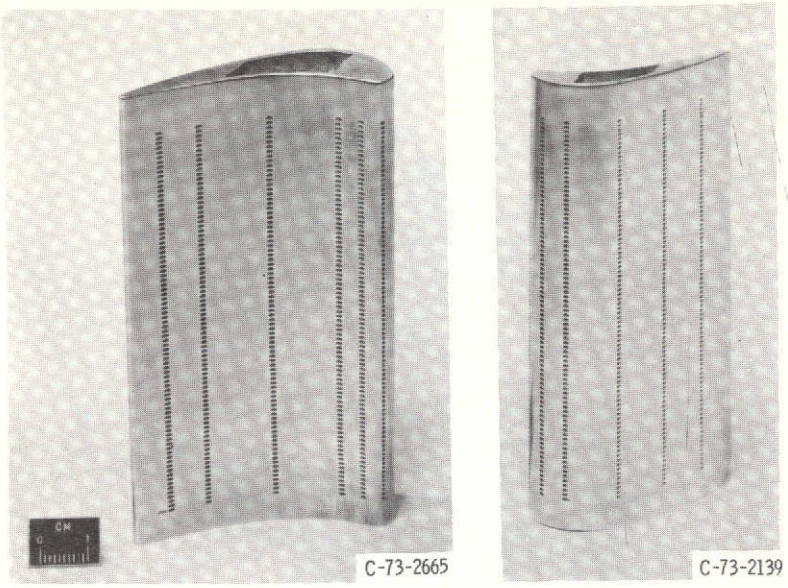

(a) Pressure-surface view. (b) Suction-surface view.

Figure 1. - Tested stator blade.

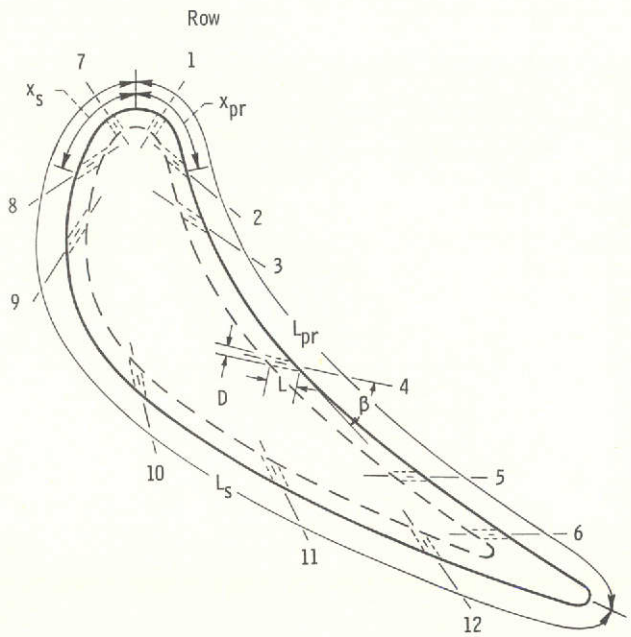

Figure 2. - Cross-sectional sketch of cooled stator blade.

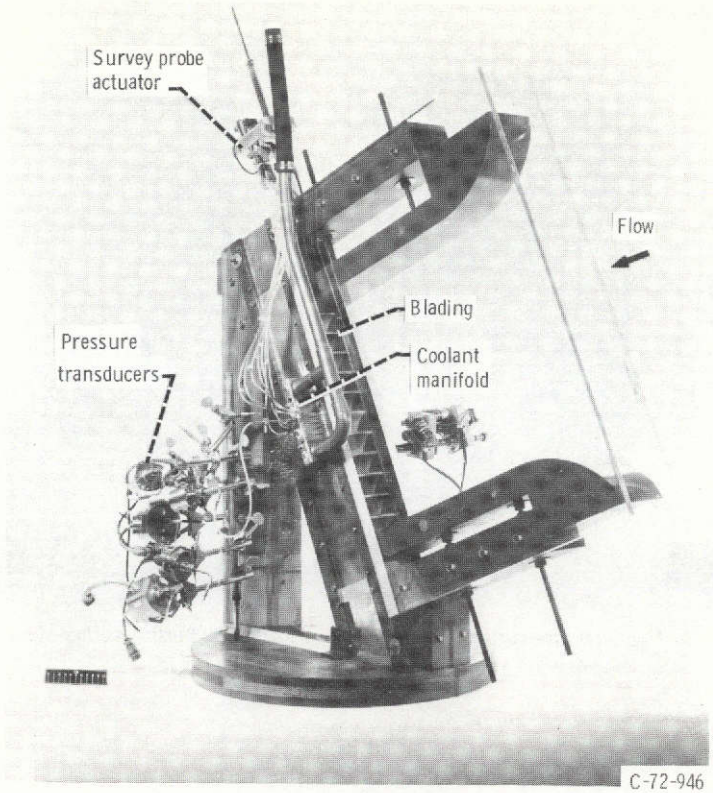

Figure 3. - Stator blade cascade.

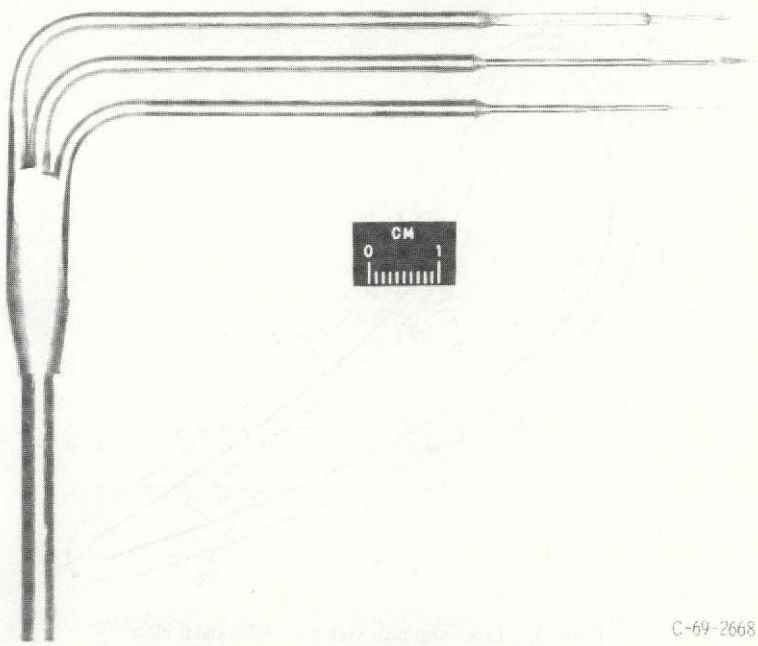

Figure 4. - Survey probe.

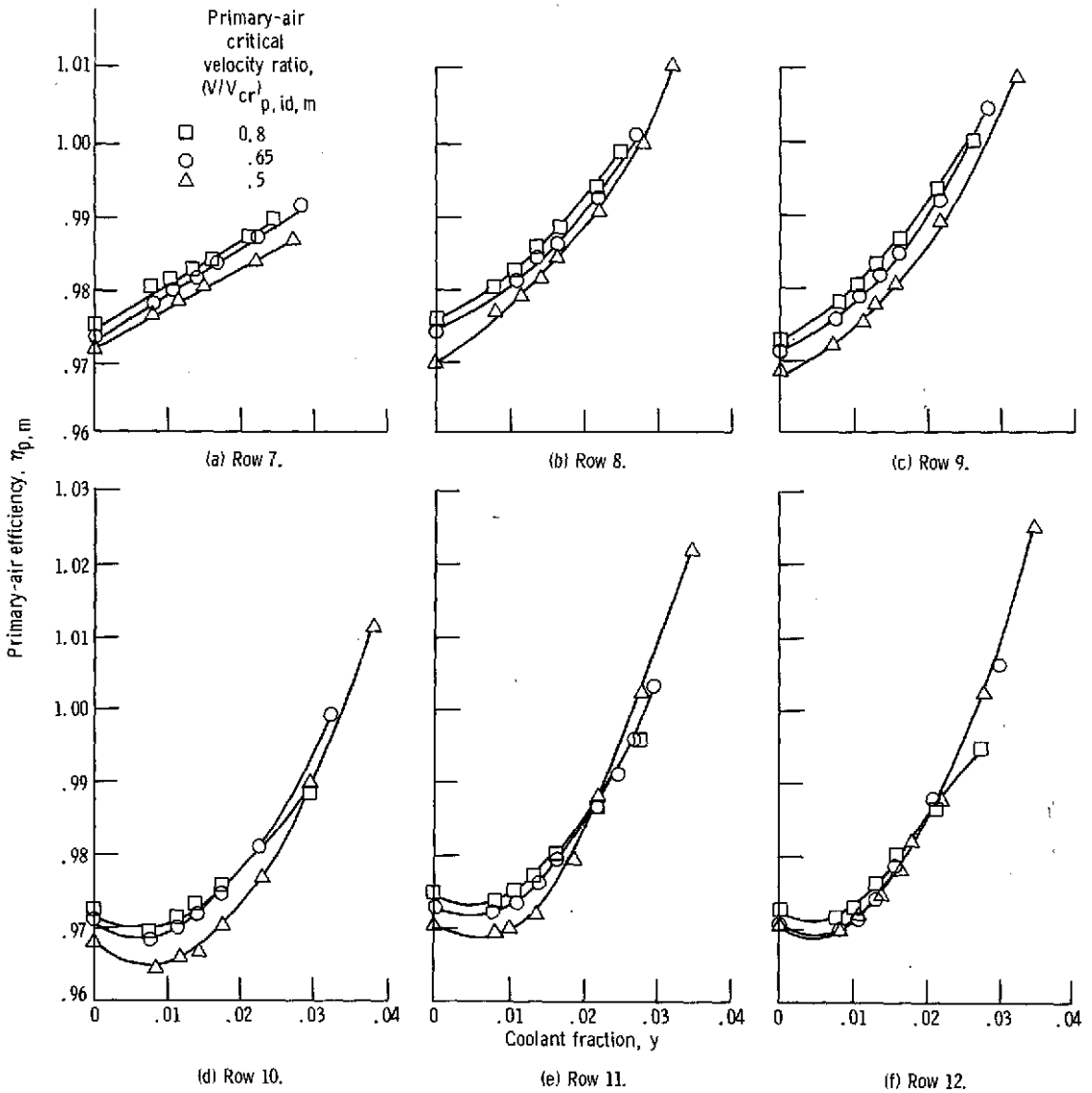

Figure 5. - Single-row variation in primary-air efficiency as function of coolant fraction and primary-air critical velocity ratio for suction-surface coolant discharge.

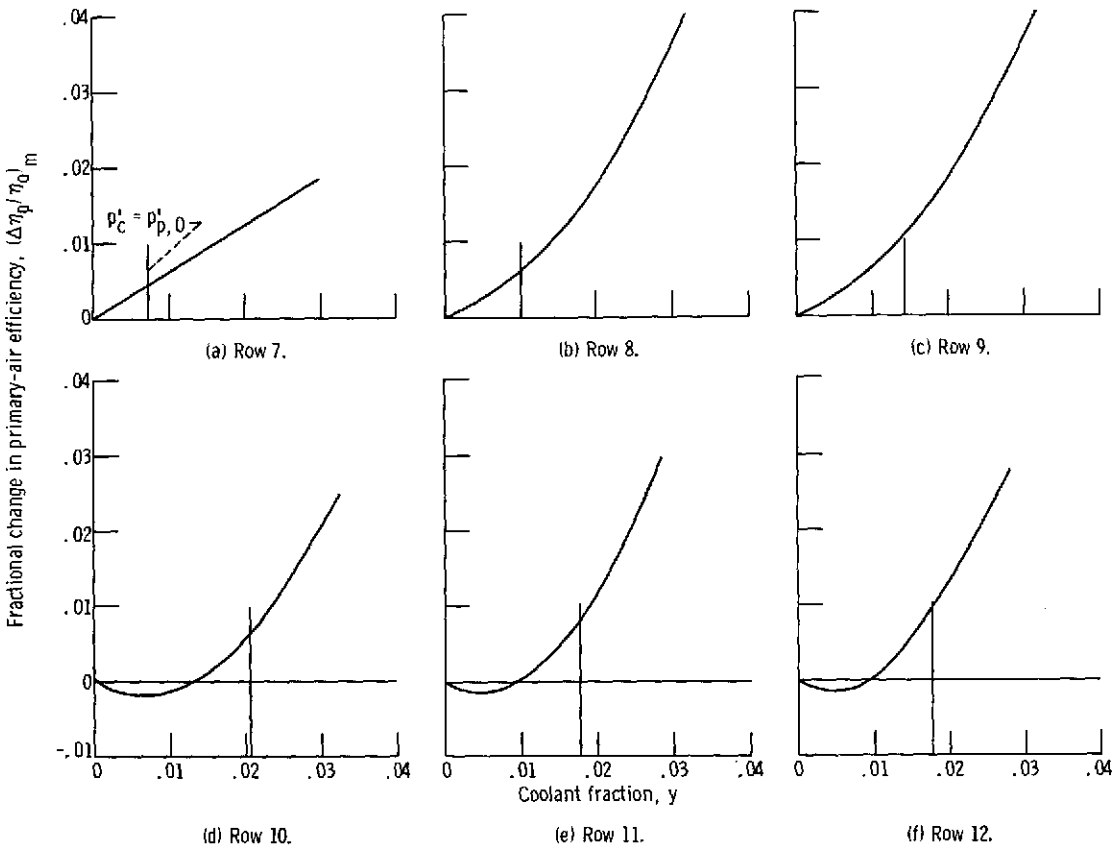

Figure 6. - Fractional variation in primary-air efficiency with coolant fraction for single-row discharge from blade suction surface. (Data averaged for primary-air critical velocity ratios from fig. 5.)

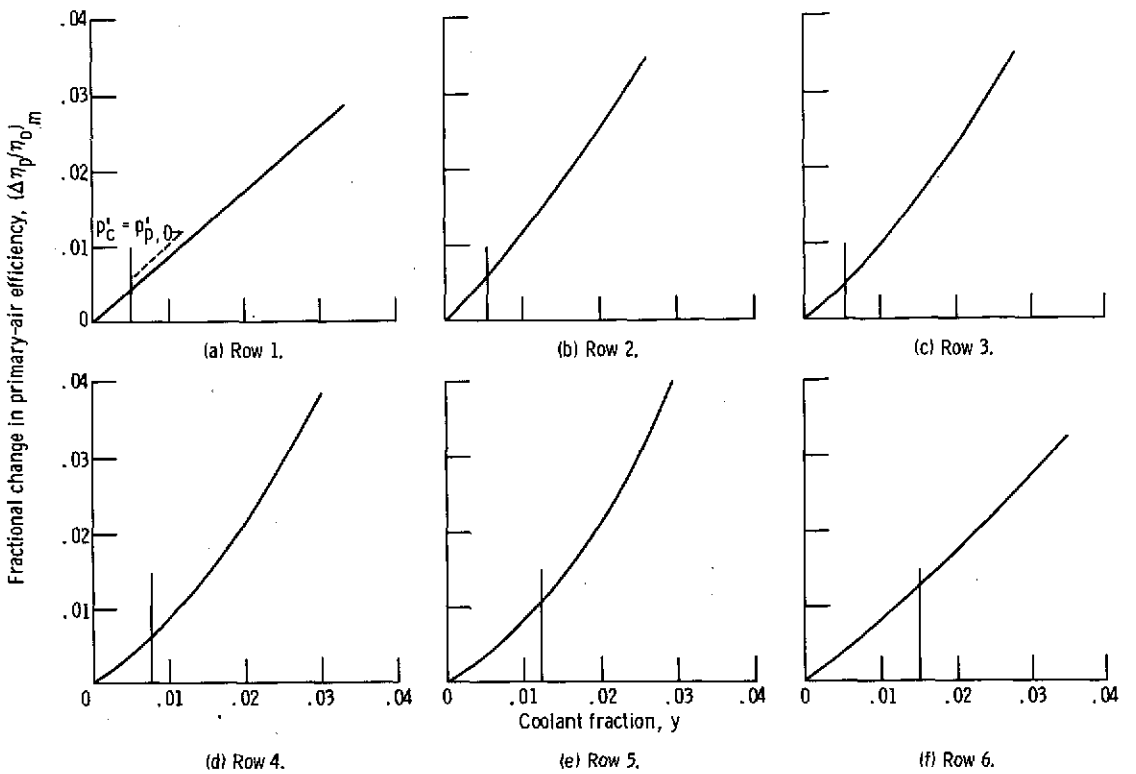

Figure 7. - Fractional variation in primary-air efficiency with coolant fraction for single-row discharge from blade pressure surface. (Data from fig. 7 of ref. 12.)

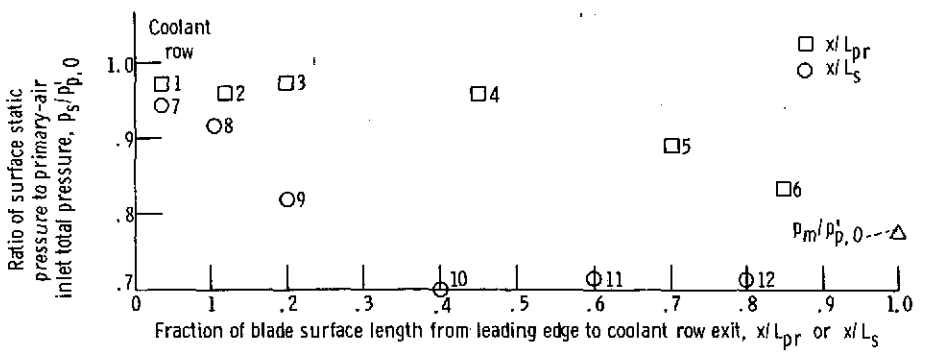

Figure 8. - Comparison of local coolant row static pressures on suction and pressure surfaces of blading for primary-air critical velocity ratio $(V/V_{cr})_{p,id,m}$ of 0.65.

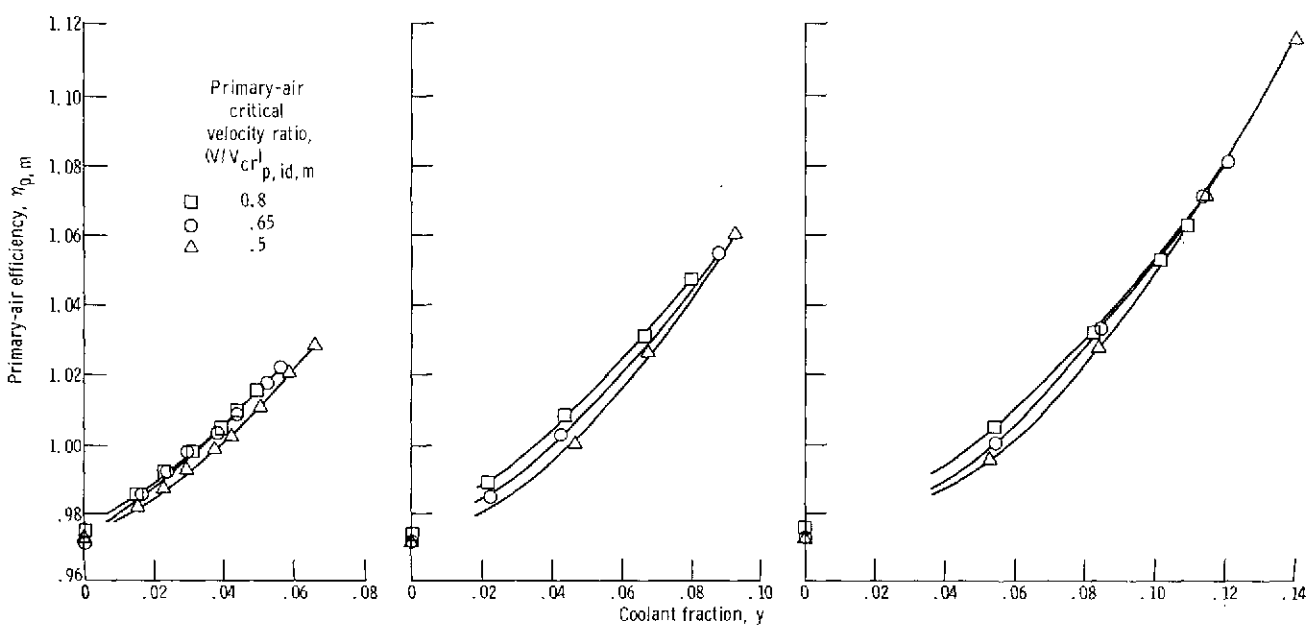

(a) Rows 7 and 8.

(b) Rows 7 to 9

(c) Rows 7 to 10.

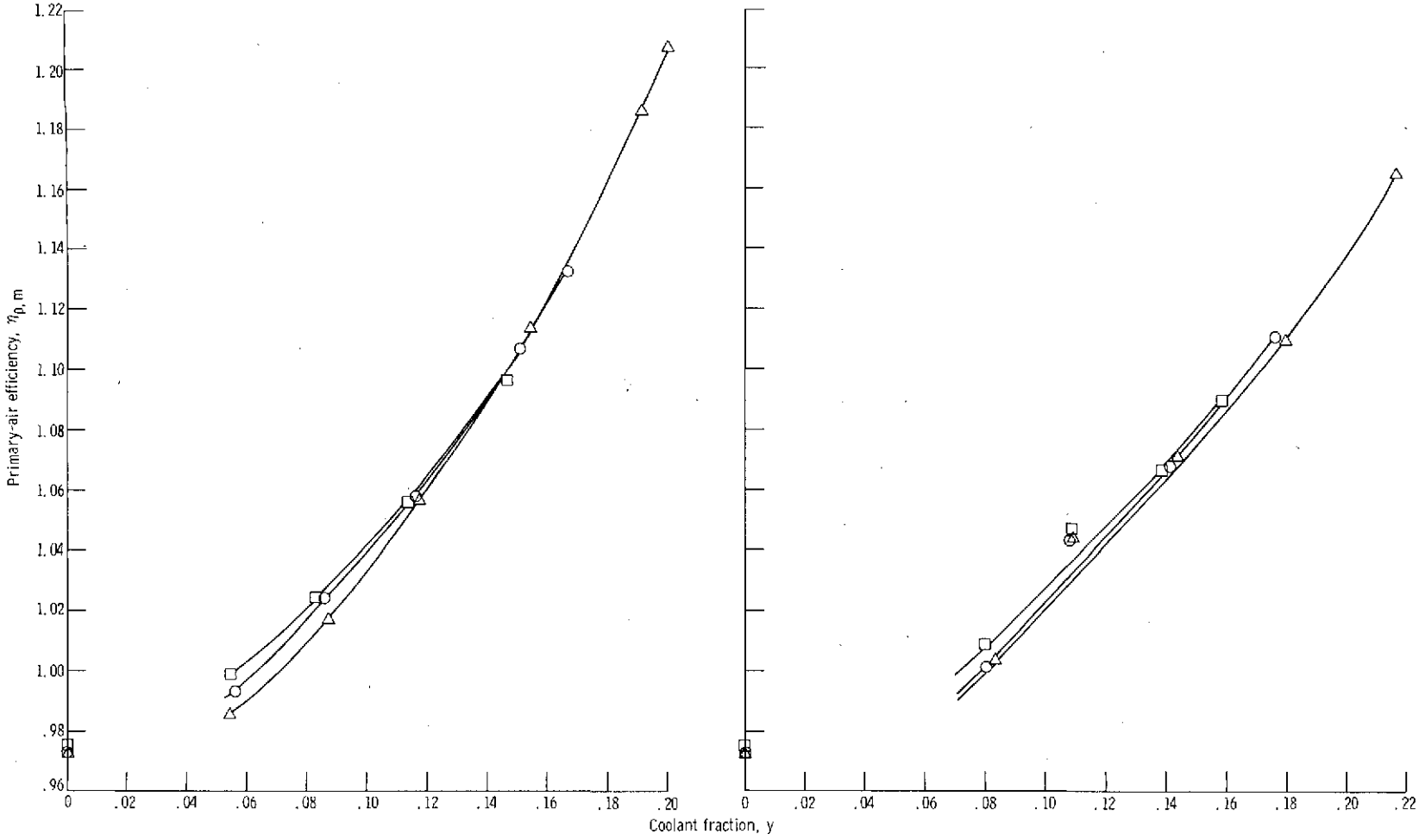

(d) Rows 7 to 11.

(e) Rows 7 to 12.

Figure 9. - Multirow variation in primary-air efficiency with coolant fraction and primary-air critical velocity ratio for suction-surface coolant discharge.

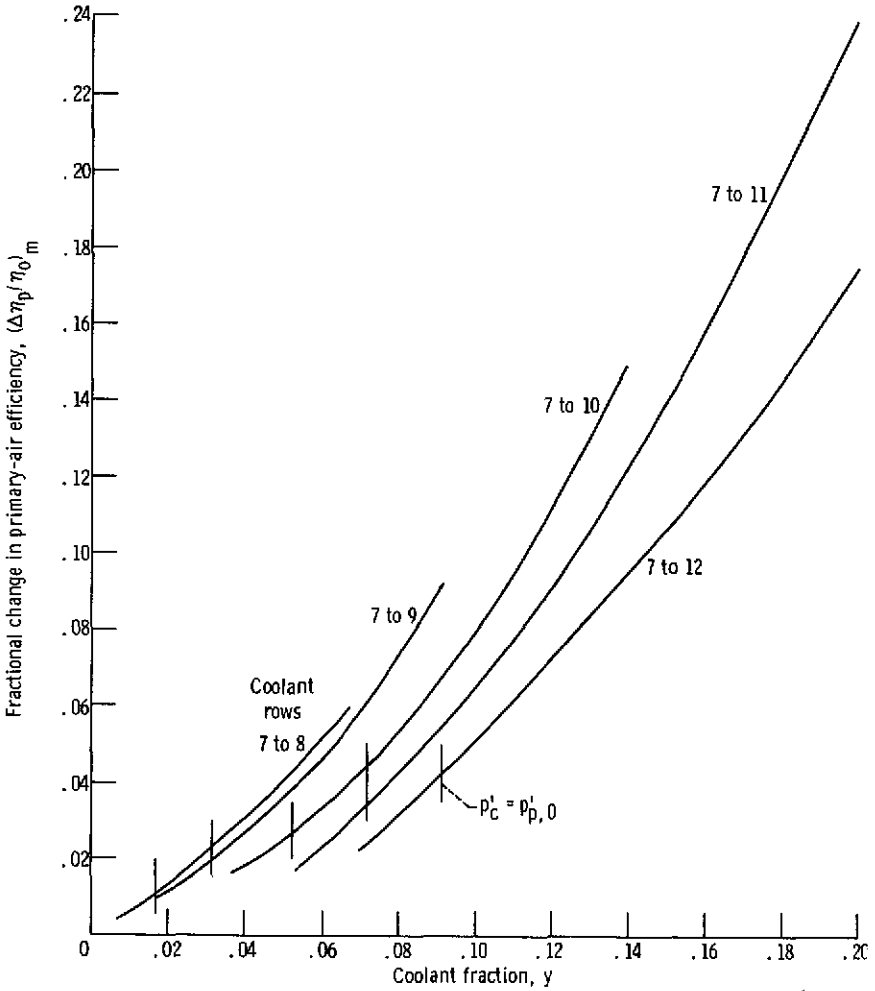

Figure 10. - Comparison of fractional variation in primary-air efficiency with coolant fraction for coolant discharge from various combinations of coolant rows on blade suction surface. (Data averaged for primary-air critical velocity ratios from fig. 9.)

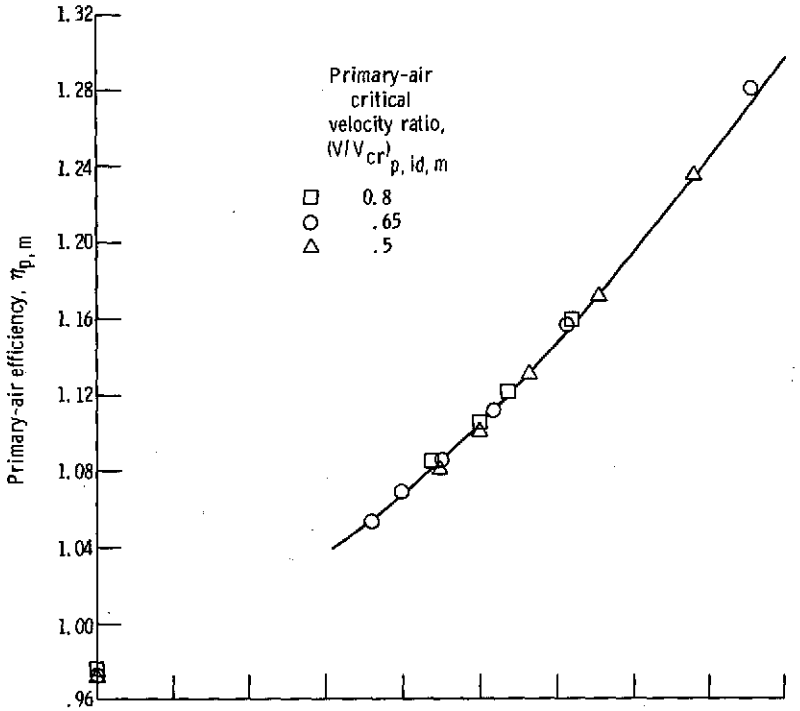

(a) Experimental efficiencies.

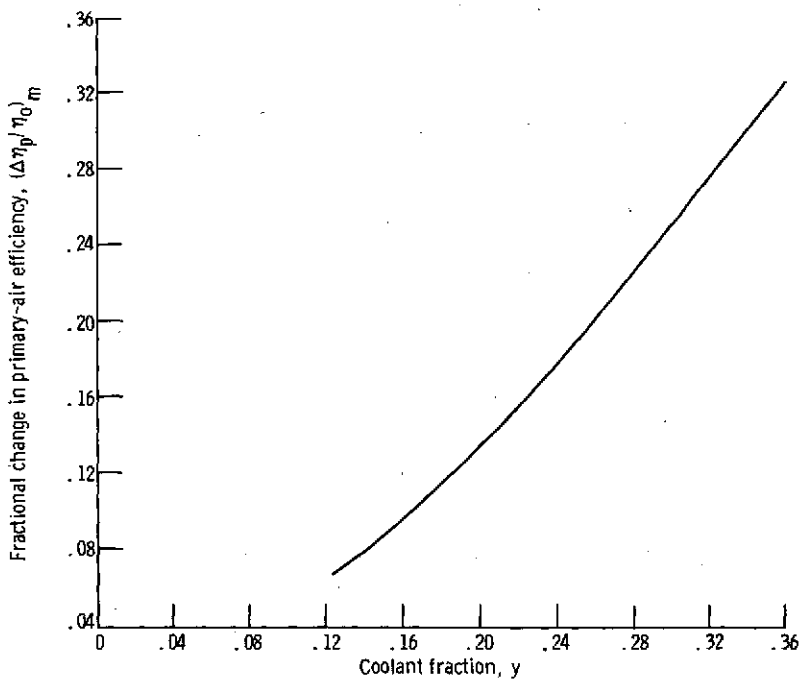

(b) Fractional variation in efficiency relative to efficiency of noncooled blading.

Figure 11. - Variation in primary-air efficiency with coolant fraction and primary-air critical velocity ratio for full film cooling. Rows 1 to 12.

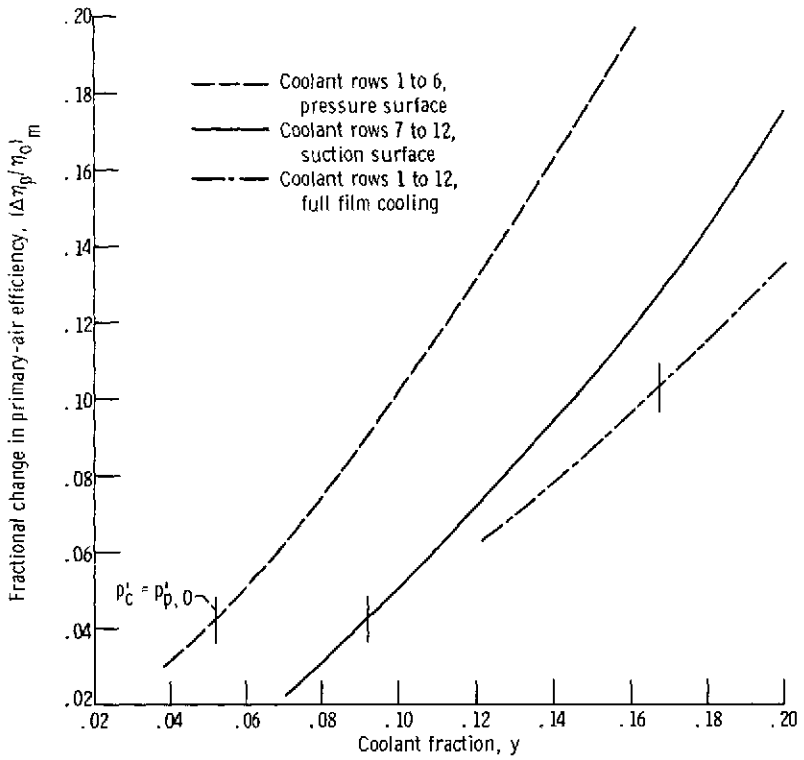

Figure 12. - Comparison of average fractional variation in primary-air efficiency with coolant fraction for coolant discharge from six rows on suction surface, coolant discharge from six rows on pressure surface, and full film cooling. (Data for pressure surface from ref. 12.)

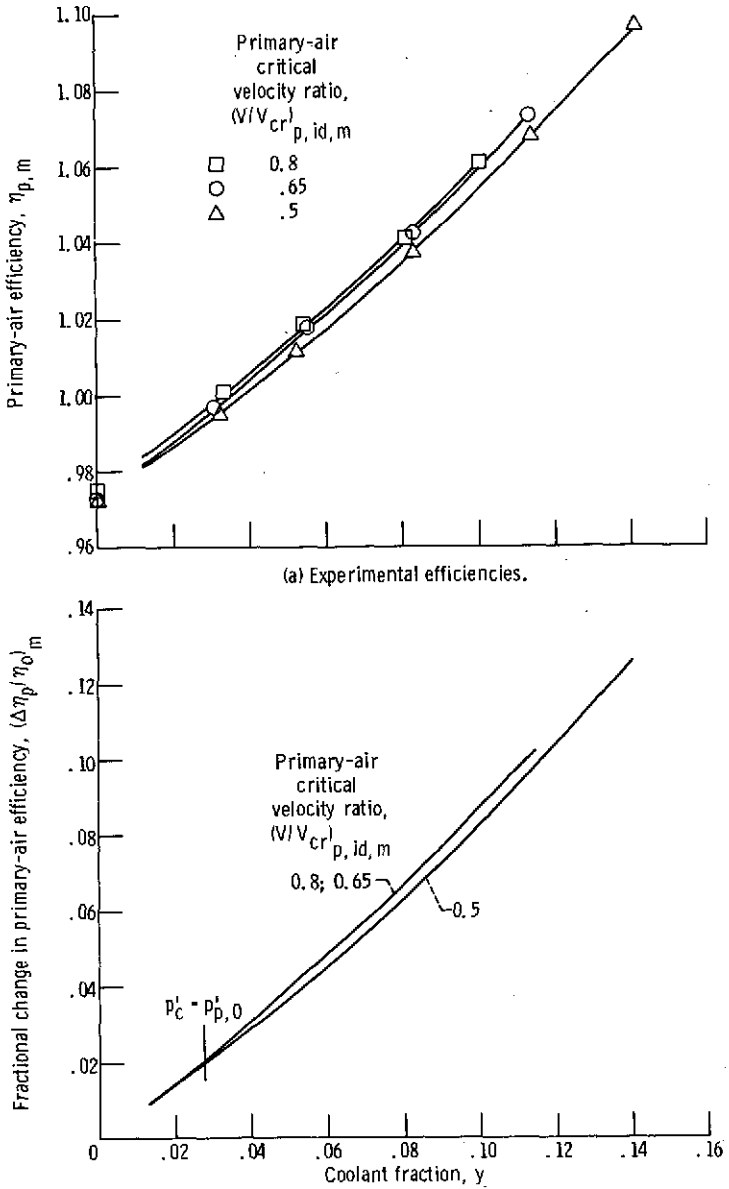

(a) Experimental efficiencies.

(b) Fractional variation in efficiency relative to efficiency of noncooled blading.

Figure 13. - Variation in primary-air efficiency with coolant fraction and primary-air critical velocity ratio for four coolant rows nearest the leading edge.

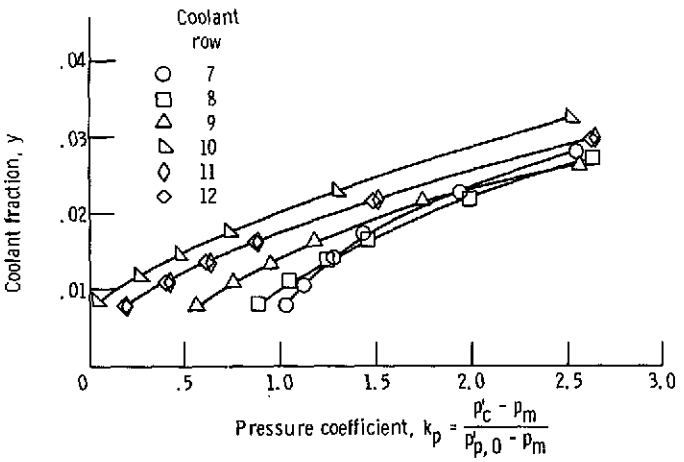

Figure 14. - Variation in single-row coolant fraction for suction-surface discharge with inlet coolant- to primary-air-pressure coefficient k_p, for a primary-air critical velocity ratio $(V/V_{cr})_{p,id,m}$ of 0.65.

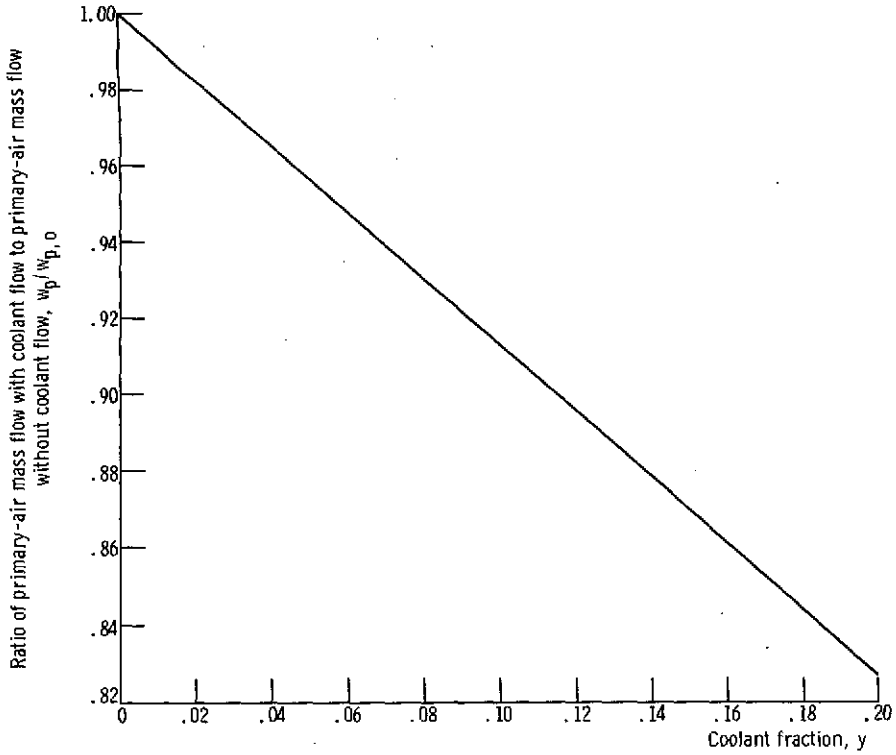

(a) Single-row and multirow coolant discharge from suction surface.

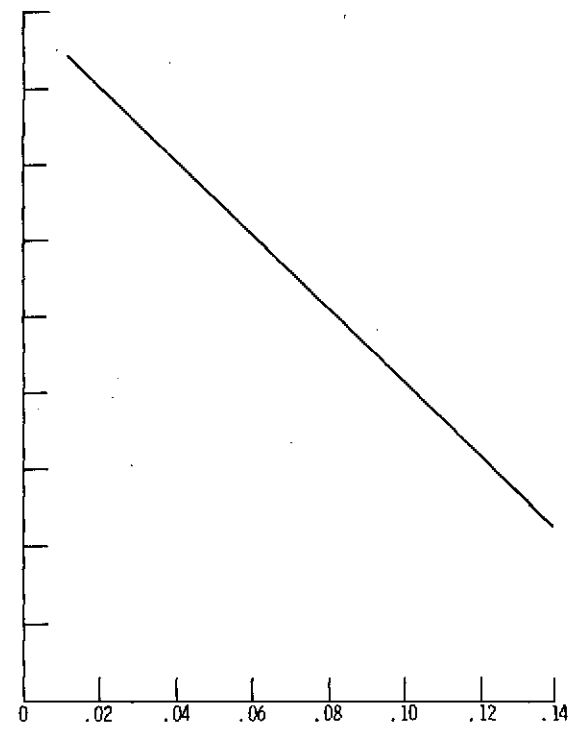

(b) Coolant discharge from four rows nearest blade leading edge.

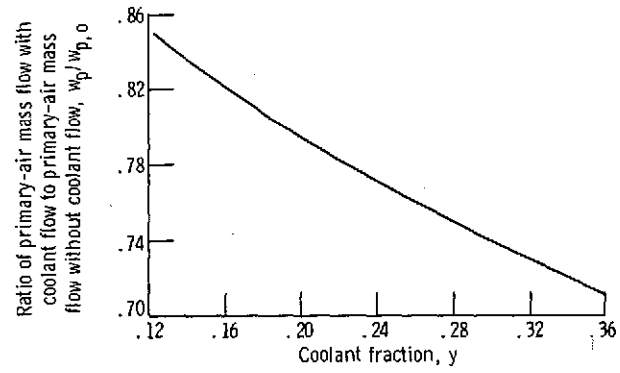

(c) Full film cooling.

Figure 15. - Effect of coolant flow on primary-air mass flow. (Data averaged for all test points.)

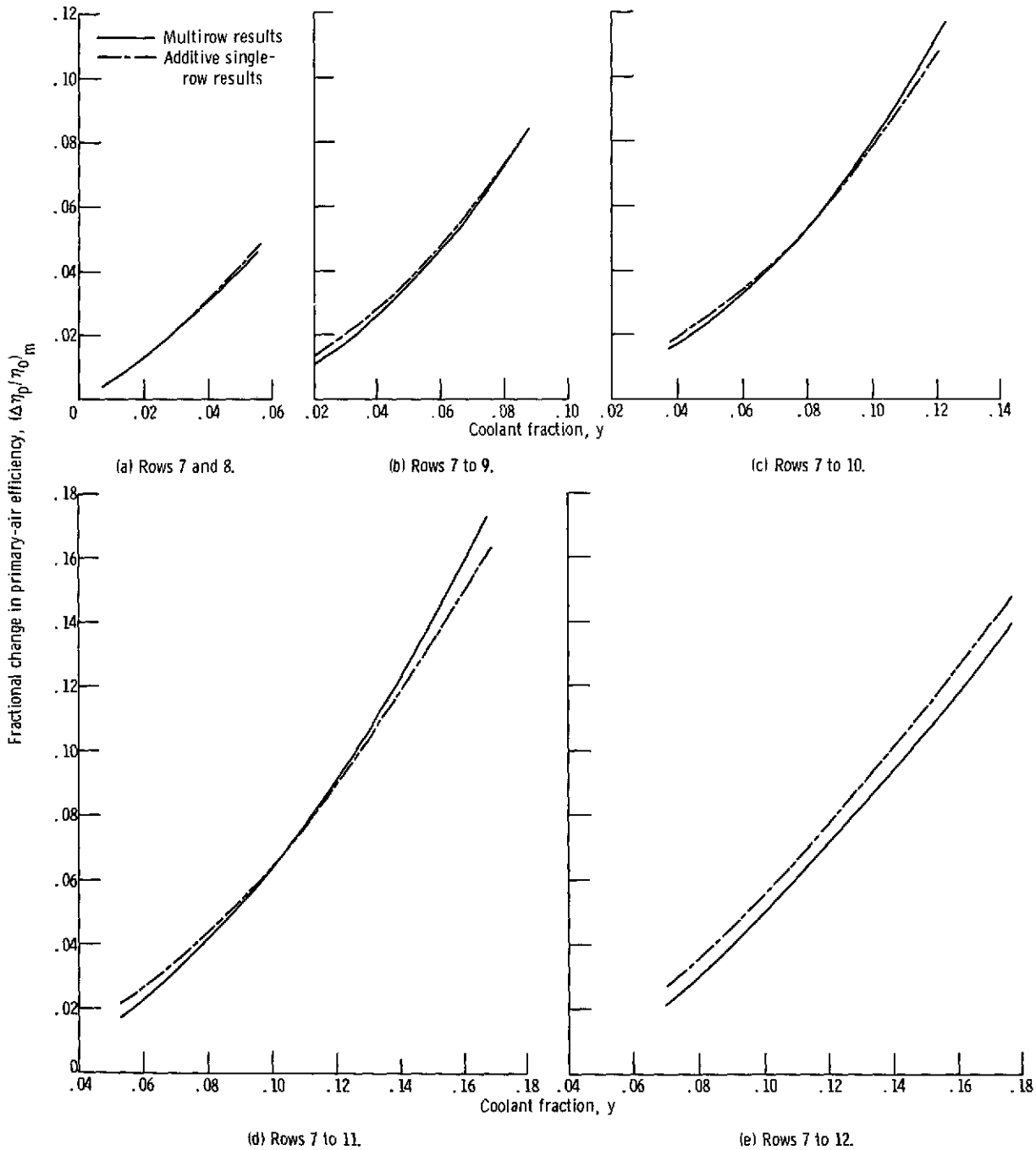

Figure 16. - Comparison of multirow results with additive single-row results for the blade suction surface. (Data averaged for primary-air critical velocity ratios.)

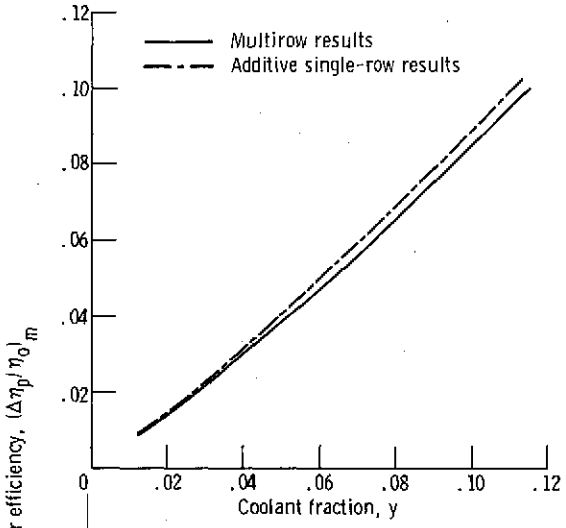

(f) Rows 1, 2, 7, and 8.

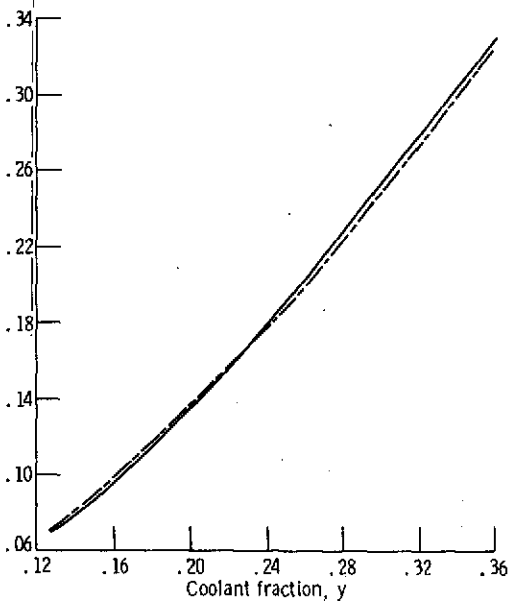

(g) Rows 1 to 12.

Figure 16. - Concluded.

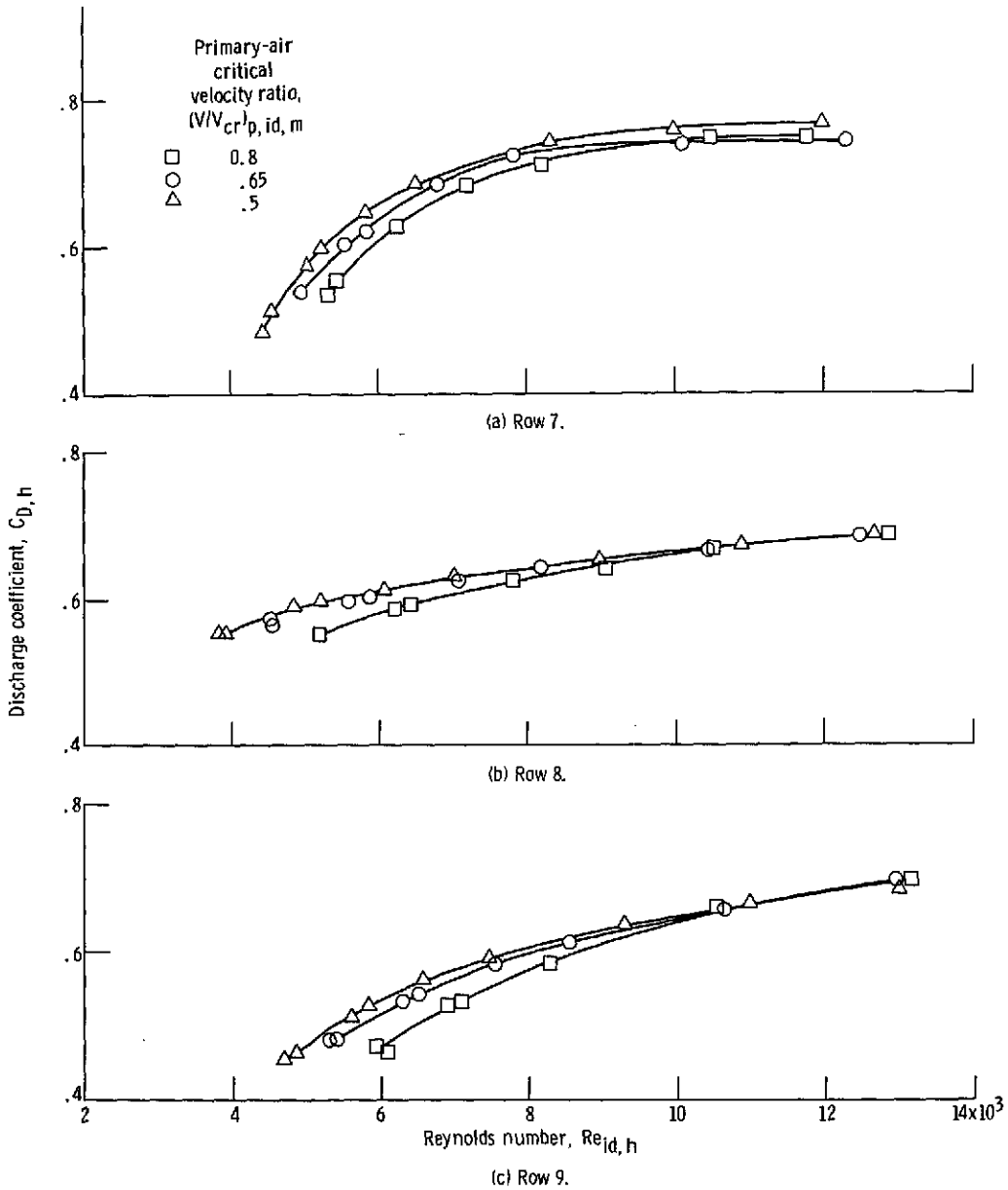

Figure 17. - Variation of discharge coefficient for suction-surface coolant holes with ideal Reynolds number and primary-air ideal exit critical velocity ratio.

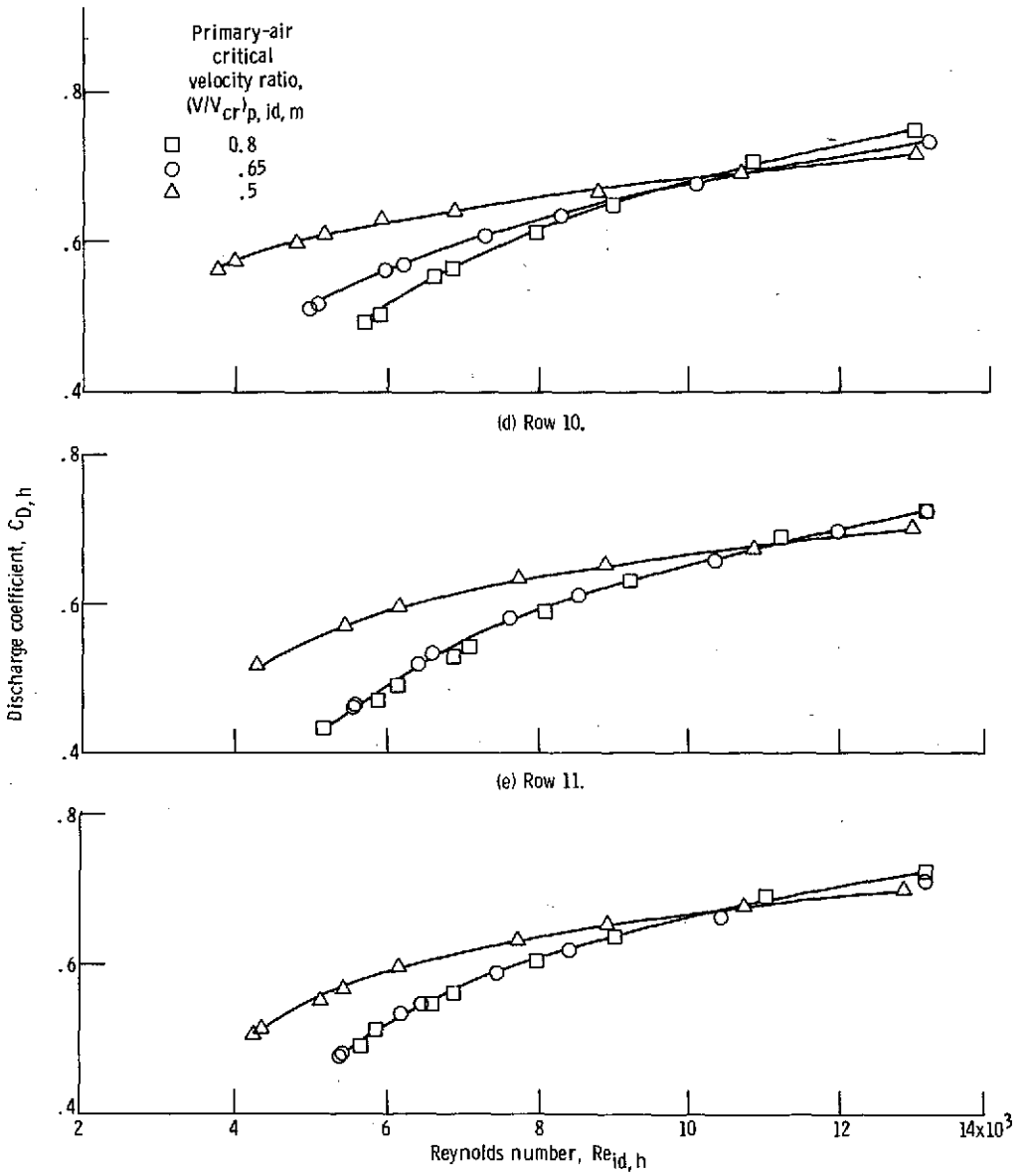

Figure 17. - Concluded.